

NMDA Receptor-Mediated Activation of NADPH Oxidase and Glomerulosclerosis in Hyperhomocysteinemic Rats

Chun Zhang, Fan Yi, Min Xia, Krishna M. Boini, Qing Zhu, Laura A. Laperle, Justine M. Abais, Christopher A. Brimson, and Pin-Lan Li

Abstract

This study investigated the role of NMDA receptor in hyperhomocysteinemia (hHcys)-induced NADPH oxidase (Nox) activation and glomerulosclerosis. Sprague–Dawley rats were fed a folate-free (FF) diet to produce hHcys, and a NMDA receptor antagonist, MK-801, was administered. Rats fed the FF diet exhibited significantly increased plasma homocysteine levels, upregulated NMDA receptor expression, enhanced Nox activity and Nox-dependent $O_2^{\cdot-}$ production in the glomeruli, which were accompanied by remarkable glomerulosclerosis. MK-801 treatment significantly inhibited Nox-dependent $O_2^{\cdot-}$ production induced by hHcys and reduced glomerular damage index as compared with vehicle-treated hHcys rats. Correspondingly, glomerular deposition of extracellular matrix components in hHcys rats was ameliorated by the administration of MK-801. Additionally, hHcys induced an increase in tissue inhibitor of metalloproteinase-1 (TIMP-1) expression and a decrease in matrix metalloproteinase (MMP)-1 and MMP-9 activities, all of which were abolished by MK-801 treatment. *In vitro* studies showed that homocysteine increased Nox-dependent $O_2^{\cdot-}$ generation in rat mesangial cells, which was blocked by MK-801. Pretreatment with MK-801 also reversed homocysteine-induced decrease in MMP-1 activity and increase in TIMP-1 expression. These results support the view that the NMDA receptor may mediate Nox activation in the kidney during hHcys and thereby play a critical role in the development of hHcys-induced glomerulosclerosis. *Antioxid. Redox Signal.* 13, 975–986.

Introduction

ALTHOUGH AT FIRST NOT GENERALLY ACCEPTED, epidemiologic studies conducted over the past 25 years have provided ample support for the association of hyperhomocysteinemia (hHcys) with an elevated risk of cardiovascular diseases such as atherothrombosis (4). There is abundant evidence showing that homocysteine (Hcys) is an atherogenic determinant that promotes oxidant stress, inflammation, thrombosis, endothelial dysfunction, and cell proliferation (11, 25, 27). Given the similarity of pathological changes between chronic glomerular injury and Hcys-induced arterial damages such as endothelial injury, cell proliferation, and increased matrix accumulation, hHcys may also play a crucial role in initiating and facilitating glomerular injury. Indeed, recent studies from our laboratory (35, 37) and by others (15) have demonstrated that Hcys could induce extracellular matrix (ECM) accumulation and inhibit their degradation in mesangial cells, which ultimately leads to glomerulosclerosis and loss of renal function. Although the detailed mechanisms

of hHcys-induced glomerulosclerosis have not been fully elucidated, we and others have demonstrated that oxidative stress mediated by NADPH oxidase (Nox) is importantly involved in the progression of glomerular injury associated with hHcys (29, 35). However, it remains unknown how Hcys exerts its action to activate Nox and results in subsequent glomerulosclerosis.

Among considerable research efforts made to identify Hcys acting sites, there are some reports indicating that the N-methyl-D-aspartate (NMDA) receptor might be a potential candidate (7). NMDA receptor is a heterotetrameric amino acid receptor, which was originally identified in the brain (7). The activation of neuronal NMDA receptor initiates several downstream events, including cation influx, activation of nitric oxide synthase, and formation of superoxide anion ($O_2^{\cdot-}$) (22). Recent studies have demonstrated that the NMDA receptor possesses a high affinity for Hcys (10, 13, 26), and Hcys has been found to bind the glutamate site of the NMDA receptor (5). This receptor also exists in brain arterial vascular bed and serves as the initial entry point for transporting Hcys

into endothelial cells (6). These studies highlighted the possibility that the NMDA receptor may serve as a Hcys acting target on the cell membrane, which mediates its action or facilitate its entry into these cells.

The NMDA receptor can also be detected in the kidney, where it exerts a tonic vasodilatory action and may account for the vasodilatory response to glycine infusion (9). Further studies demonstrated that NMDA receptor subunits, NR1 and NR2C, are expressed in renal tubular epithelial cells (18) and may be involved in the regulation of tubular reabsorption and glomerular filtration (8). In gentamicin-induced nephrotoxicity, increased expression of NR1 has been demonstrated to be present in renal tubules and the application of a NMDA receptor antagonist efficiently ameliorated tubular injury (17), suggesting a detrimental response caused by NMDA receptor upregulation in renal tissues. In a very recent study, it was found that NMDA receptor was also expressed by glomerular cells, particularly glomerular epithelial cells [*i.e.*, podocytes (14)]. However, the role of NMDA receptor in Nox activation and its possible role in the pathogenesis of hHcys-induced glomerulosclerosis remain unclarified.

In the present study, we hypothesized that the NMDA receptor may play an essential role in mediating hHcys-induced Nox activation and consequent glomerulosclerosis. To test this hypothesis, we first characterized the expression of NMDA receptor subunits in rat kidney tissue sections. Then, we examined whether the expression of the NMDA receptor is changed in hHcys rat glomeruli. Mechanistically, we investigated the role of NMDA receptor in Nox-dependent $O_2^{\cdot-}$ production, glomerular ECM accumulation, and subsequent development of glomerulosclerosis during hHcys. In addition, cultured rat mesangial cells were stimulated with Hcys to explore the cellular mechanisms of mesangial ECM accumulation through the NMDA receptor. In these experiments, dizocilpine maleate (MK-801), a noncompetitive antagonist for the NMDA receptor, was used to block the possible effects of hHcys and to further delineate the role of NMDA receptor in mediating Nox activation and glomerular injury.

Materials and Methods

Animal procedures

Animal experiments were performed using Sprague-Dawley rats (8-weeks-old) purchased from Harlan Inc. (Madison, WI). To speed up the damaging effects of hHcys on glomeruli, all rats were uninephrectomized as described in several previous studies by us (35) and others (28). After a 1-week recovery period from the uninephrectomy, rats were maintained on a normal diet or a folate-free (FF) diet (Dyets Inc, Bethlehem, PA) for 6 weeks with or without subcutaneous injection of MK-801 (Sigma, St. Louis, MO) at a dosage of 0.15 mg/kg, twice a week ($n = 18$ per group). The dose of MK-801 was chosen according to recent reports (8, 17) and our preliminary experiments that tested dose-dependence. In additional experiments, rats were given methionine in their drinking water at a dosage of 1.0 g/kg.d for 6 weeks to induce hHcys as we reported before (34), with and without the injection of MK-801 ($n = 12$ per group). All protocols were approved by the Institutional Animal Care and Use Committee of the Virginia Commonwealth University. Mean arterial pressure (MAP) and heart rate were measured using telemetry transmitters in conscious rats as we described previously

(19) at the sixth week of different treatments. One day before these rats were sacrificed, 24-h urine samples were collected using metabolic cages. After blood samples were collected, these rats were sacrificed and renal tissues were harvested for biochemical and molecular analyses as well as morphological examinations. Hematocrit, creatinine clearance, and urine albumin excretion were measured as we reported previously (19, 38). Lipid peroxidation product (*i.e.*, malondialdehyde plus 4-hydroxylakenals (MDA + 4-HA)) concentration was detected by a colorimetric assay using a commercially available kit (Oxford Biomedical Research, Oxford, MI).

Culture of rat mesangial cells

The rat mesangial cell line was obtained from the American Type Culture Collection (ATCC, Manassas, VA) and maintained in Dulbecco's modified Eagle's medium containing 18 mM sodium bicarbonate, 25 mM glucose, and 10% fetal bovine serum with 4 mM of L-glutamine at 37°C in 5% CO_2 atmosphere. In the present study, the preparation of L-Hcys (a pathogenic form of Hcys) and the concentration of L-Hcys treatment were chosen based on our previous studies (36). After rat mesangial cells were pretreated with or without MK-801 (200 μM) for 2 h, they were incubated with the vehicle or L-Hcys for 24 h. Then, $O_2^{\cdot-}$ production, MMP-1 activity, and TIMP-1 expression were examined as described below.

High-performance liquid chromatography analysis

Plasma Hcys levels were measured using high-performance liquid chromatography (HPLC) method as we described previously (36). Briefly, blood samples were centrifuged at 1000 g for 10 min at 4°C to isolate the plasma. A 100 μl of plasma or standard solution was treated with 10 μl of 10% tri-n-butylphosphine solution in dimethylformamide at 4°C for 30 min. Then, 80 μl ice-cold 10% trichloroacetic acid in 1 mM EDTA was added and centrifuged to remove proteins in the sample. 100 μl of the supernatant were transferred into the mixture of 20 μl of 1.55 M sodium hydroxide, 250 μl of 0.125 M borate buffer (pH 9.5), and 100 μl of 1.0 mg/mL ABD-F solution. The resulting mixture was incubated at 60°C for 30 min to accomplish derivatization of plasma thiols. HPLC was performed with a HP 1100 series equipped with a binary pump, a vacuum degasser, a thermostated column compartment, and an autosampler (Agilent Technologies, Waldbronn, Germany). Separation was carried out at an ambient temperature on an analytical column. Fluorescence intensities were measured with an excitation wavelength of 385 nm and emission wavelength of 515 nm. The peak area of the chromatographs was quantified with a Hewlett-Packard 3392 integrator. The analytical column was eluted with 0.1 M potassium dihydrogen phosphate buffer (pH 2.1) containing 6% acetonitrile (v/v) as the mobile phase with a flow rate of 2.0 ml/min.

Morphological examinations

The perfusion was performed using a roller pump. Pre-fixation perfusion using phosphate buffer was done prior to fixation to ensure removal of blood. Then, 4% paraformaldehyde was used to perfuse the kidneys at a speed of 10 ml/min for 15 min. After a post-fixation with 4% paraformaldehyde, the tissues were embedded and sliced. The slices

were stained with periodic acid-Schiff (PAS) or Masson trichrome. Glomerulosclerosis was assessed by a standard semiquantitative analysis and expressed as glomerular damage index (GDI), as we described before (37). Tubulo-interstitial fibrosis was evaluated by Masson staining and the data were presented as fibrosis area/total tubulo-interstitial area.

Immunohistochemistry

The kidneys were embedded with paraffin and 5 μm slices were cut from the embedded blocks. After performing heat-induced antigen retrieval, slides were incubated with primary antibodies diluted in phosphate-buffered saline (PBS). Anti-NR1 (Cell Signaling, Danvers, MA; 1:100), anti-NR2A (Zymed, South San Francisco, CA; 1:50), anti-NR2B (Zymed, South San Francisco, CA; 1:50), and anti-TIMP-1 (R&D system, Minneapolis, MN) antibodies were used in this study. After incubation with each of these primary antibodies overnight, the sections were washed in PBS and incubated with biotinylated IgG (1:250) for 1 h and then with streptavidin-HRP for 30 min at room temperature. Then, 50 μl of DAB was added to each kidney sections and stained for 1–5 min. After washing, the slides were counterstained with hematoxylin for 5 min. The slides were then mounted and observed under a microscope in which photos were taken. Glomerular stainings of NR1, NR2A, and TIMP-1 were quantified by the Image Pro Plus 6.0 software (Media Cybernetics, Bethesda, MD) and the data were normalized to vehicle-treated rats on the normal diet. A minimum of thirty glomeruli in five consecutive nonoverlapping cortical fields were used for analysis in each slide.

Sirius red staining

To detect collagen deposition in the glomeruli, kidney sections were stained with Sirius red as described previously (20). In brief, sections were dewaxed and incubated with 0.1% Sirius red in aqueous picric acid for 2 h. Slides were washed in tap water, dried, and then mounted. Using this method, collagens were stained a red color. The slides were observed by a blinded observer, and 20 glomerular photos were randomly taken at a magnification of X400 in each kidney section. Collagen staining in the glomeruli was calculated according to positively-stained area/total glomerular area using the Image Pro Plus 6.0 software.

Isolation of glomeruli

Glomeruli were isolated by the sieving method. Briefly, kidneys were flushed with ice-cold Krebs–Henseleit–saline (KHS) buffer via an aortal catheter. Minced renal cortex was passed through three steel sieves (300, 150, and 75 μm), using ice-cold KHS buffer, and glomeruli were recovered from the 75- μm sieve, washed, and resuspended at 4°C. By light microscopy, purity of glomeruli was more than 95% in all preparations. The glomeruli were collected and stored in 80°C refrigerator for further use.

Western blot analysis

Protein was collected using sucrose buffer and run into SDS-PAGE gel, transferred into PVDF membrane, and blocked. Then, the membrane was probed with primary antibodies of anti-NR1, anti-NR2A, anti-MMP-1, anti-MMP-9

(1:500 dilution; Cell Signaling Technology, Inc., Danvers, MA), and anti-TIMP-1 (1:1000 dilution; R&D systems, Minneapolis, MN) overnight at 4°C, followed by incubation with horseradish peroxidase-labeled immunoglobulin G. The immunoreactive bands were detected by chemiluminescence methods and visualized on Kodak Omatic film. β -Actin was probed to serve as a loading control. The intensity of the bands were quantified by densitometry and normalized to the control group.

Nox activity assay

A dihydroethidium (DHE)-based fluorescence spectrometric assay was used to assess Nox activity as we described before (37). Briefly, glomerular protein (10 μg) was incubated with 1 mM of NADPH for 5 min at 37°C. Then, 100 μM of DHE and 0.5 mg/ml of salmon testes DNA (binding with ethidium to amplify fluorescence signal) were added and the ethidium fluorescence was recorded using a fluorescence microplate reader (FLX800, Bio-Tek, Winooski, VT). Ethidium fluorescence intensity was used to represent Nox activity and the data were expressed as percent changes of Nox activity compared with vehicle-treated rats on the normal diet.

Electromagnetic spin resonance analysis of Nox-dependent $\text{O}_2^{\cdot-}$ production

For detection of Nox-dependent $\text{O}_2^{\cdot-}$ production, proteins from isolated glomeruli or *in vitro* cultured rat mesangial cells were extracted using sucrose buffer and resuspended with modified Krebs–Hepes buffer containing deferoximine (100 μM , Sigma) and diethyldithiocarbamate (5 μM , Sigma). The Nox-dependent $\text{O}_2^{\cdot-}$ production was examined by addition of 1 mM NADPH as a substrate in 50 μg protein and incubated for 15 min at 37°C in the presence or absence of SOD (200 U/ml), and then supplied with 1 mM $\text{O}_2^{\cdot-}$ specific spin trap 1-hydroxy-3-methoxycarbonyl-2,2,5,5-tetramethylpyrrolidine (CMH, Noxygen, Elzach, Germany). The mixture was loaded in glass capillaries and immediately analyzed for $\text{O}_2^{\cdot-}$ production kinetically for 10 min in a Miniscope MS200 electromagnetic spin resonance (ESR) spectrometer (Magnettech Ltd, Berlin, Germany). The ESR settings were as follows: biofield, 3350; field sweep, 60 G; microwave frequency, 9.78 GHz; microwave power, 20 mW; modulation amplitude, 3 G; 4,096 points of resolution; receiver gain, 20 for tissue and 50 for cells. The results were expressed as the fold changes of control.

Real-time reverse transcription polymerase chain reaction

Total RNA from rat glomeruli and cultured mesangial cells were isolated using TRIzol reagent (Invitrogen, Carlsbad, CA). RNA samples were quantified by measurement of optic absorbance at 260 nm and 280 nm in a spectrophotometer. The concentrations of RNA were calculated according to A260. Aliquots of total RNA (1.0 μg) from each sample were reverse-transcribed into cDNA according to the instructions of the first strand cDNA synthesis kit manufacturer (Bio-Rad, Hercules, CA). Equal amounts of the reverse transcriptional products were subjected to real-time polymerase chain reaction (PCR) amplification using SYBR Green as a fluorescence indicator on a Bio-Rad iCycler system (Bio-Rad, Hercules, CA). The

primers used in this study were synthesized by Operon (Huntsville, AL) and the sequences were: matrix metalloproteinase (MMP)-1 sense TCAAGGAGGTGATGGATGAA, antisense CCACACATGGGTGTCTTGAT; MMP-2 sense CTGATAACCTGGATGCAGTCGT, antisense CCAGCCAGTCCGATTGTA; MMP-9 sense CTGCAGTGCCCTTGAATAA, antisense TATCCGGCAAAGTAGCTCCT; tissue inhibitor of metalloproteinase-1 (TIMP-1) sense TCTGGCATCCTCTTGTGCTAT, antisense CCACAGCGTCGAA TCCTT; β -actin sense ACAGAAGCAATGCTGTCACC, antisense CAATGTGGCTGAGGACTTTG. The mRNA levels of the target genes were normalized to the β -actin mRNA levels detected from the same samples.

Fluorescence resonance energy transfer assay of MMP activities

Glomerular MMP-1, MMP-2, and MMP-9 activities were measured using EnzoLyte™ 520 MMP-1 assay kit from AnaSpec Inc. (San Jose, CA). This kit uses a 5-FAM (fluorophore)- and QXL520™ (quencher)-labeled fluorescence resonance energy transfer (FRET) peptide substrate for continuous measurement of the enzyme activities. In an intact FRET peptide, the fluorescence of 5-FAM was quenched by QXL520™. Upon cleavage of the FRET peptide by MMP-1, the fluorescence of 5-FAM was recovered and could be continuously monitored at excitation/emission (490/520 nm). MMP activities were measured according to the protocol described by the manufacturer. The changes of MMP activities were presented as percent change in relative fluorescence unit *vs.* control.

Statistical analysis

Results are expressed as mean \pm SEM. Significant differences among groups were assessed by one-way ANOVA, followed by a Duncan's multiple comparison post test using SigmaStat 3.5 software (Systat Software, Inc. Chicago, IL).

χ^2 test was used to assess the significance of ratio and percentage data. $P < 0.05$ was considered statistically significant.

Results

Characterization of NMDA receptor subunits in rat kidneys

The present study first characterized the expression of NMDA receptor subunits including NR1, NR2A, and NR2B in normal rat kidneys using immunohistochemistry. It was found that both NR1 and NR2A receptors were expressed in the glomeruli. In the medulla, NR1 receptor was mainly detected in thin limb cells and some distal tubular epithelial cells, while NR2A was expressed by vascular endothelial cells and interstitial cells. However, NR2B was not detected in either the renal cortex or the medulla (Fig. 1).

Increased NR1 and NR2A expression in the glomeruli of rats on the FF diet

HPLC analysis showed that plasma Hcys levels significantly increased in uninephrectomized rats exposed to a 6-week FF diet treatment (Fig. 2A), which indicated a successful establishment of the hHcys model. MK-801 treatment did not influence the basal level of Hcys and had no effect on the increase in Hcys levels induced by the FF diet. As shown in Table 1, the values of some basic physiological parameters, such as body weight, heart rate, MAP, hematocrit, and urine output did not show any significant changes upon FF diet treatment. Interestingly, NR1 and NR2A expressions were significantly increased in the glomeruli of FF diet-treated rats, which were attenuated by the treatment with MK-801 (Figs. 2B and 2C). Similar expression patterns of NR1 and NR2A in the glomeruli of these rats were also confirmed by Western blot analysis (Supplemental Fig. 1; see www.liebertonline.com/ars).

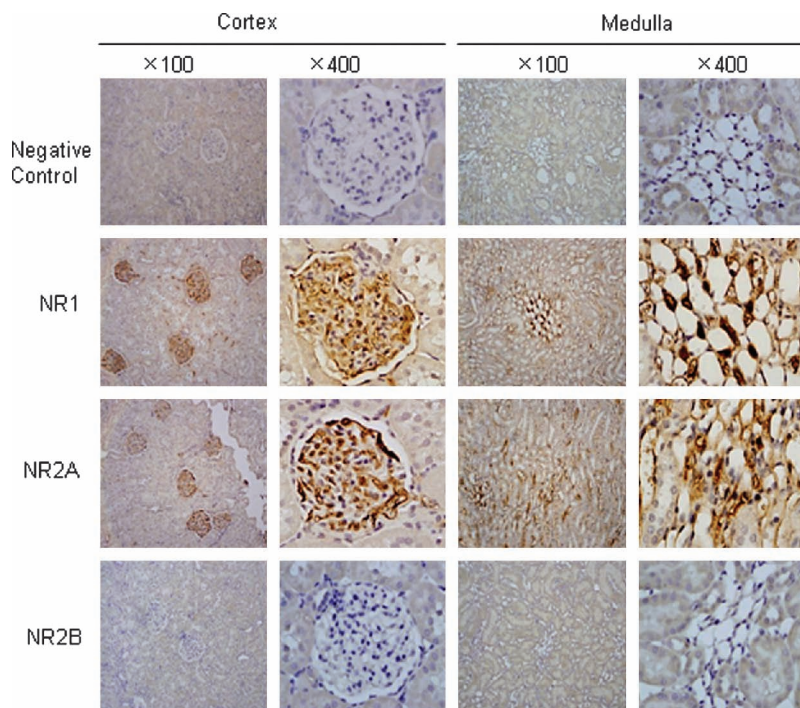


FIG. 1. Identification and characterization of NMDA receptor subunits in rat kidneys. Immunohistochemical staining shows the expression pattern of NR1, NR2A, and NR2B in the renal cortex and medulla. (Original magnification, X100, X400). (For interpretation of the references to color in this figure legend, the reader is referred to the web version of this article at www.liebertonline.com/ars).

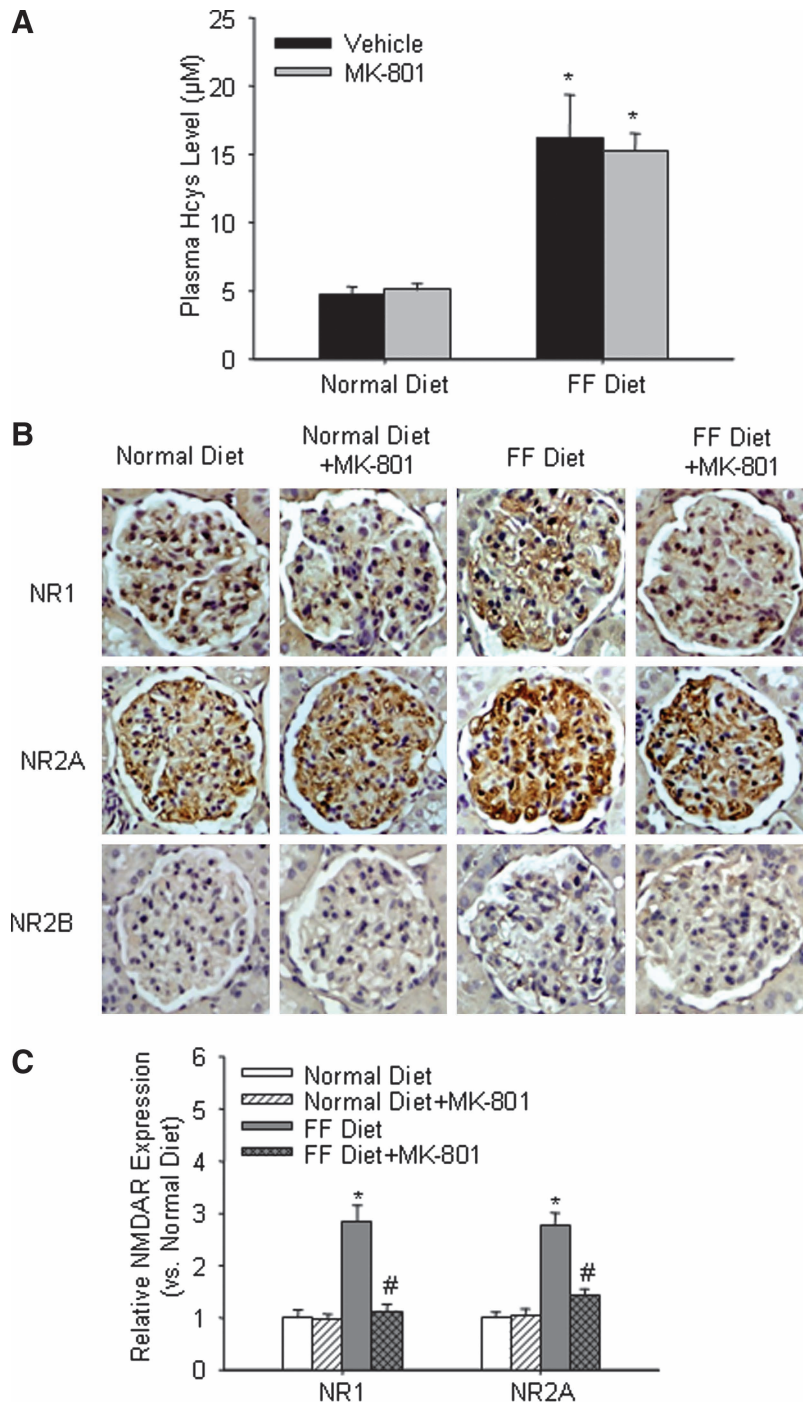


FIG. 2. Effects of folate-free (FF) diet on plasma Hcys levels and NMDA receptor expressions in rat glomeruli. (A) Plasma Hcys levels in four groups of rats measured by HPLC ($n = 10$). (B) A representative immunohistochemistry image showing the expression of NR1 and NR2A in the glomeruli of different groups of rats (original magnification, X400; $n = 6$ per group). (C) Relative quantitation of NR1 and NR2A expressions in immunohistochemical staining. Image Pro Plus 6.0 software was used to quantify NR1 and NR2A staining in the glomeruli. A minimum of 30 glomeruli were analyzed for each section. Data was normalized to rats on the normal diet and the fold changes were compared. $N = 6$ per group. * $p < 0.05$ vs. rats on the normal diet; # $p < 0.05$ vs. vehicle-treated rats on the FF diet. (For interpretation of the references to color in this figure legend, the reader is referred to the web version of this article at www.liebertonline.com/ars).

.com/ars). However, NR2B expression was not detectable in the kidneys of rats on either normal and FF diets.

Treatment with MK-801 reduced Nox activation, Nox-dependent O₂⁻ production, and lipid peroxidation in the glomeruli of hHcys rats

DHE assay showed that Nox activity was significantly increased in the glomeruli from FF diet-treated rats, which was substantially reduced by the treatment with MK-801 (Fig. 3A). As shown in Figure 3B, the ESR spectrometric curve exhibited significantly increased amplitude of Nox-dependent O₂⁻

signals in the glomeruli isolated from rats on the FF diet as compared with rats on the normal diet. Although MK-801 had no obvious effect on glomerular O₂⁻ production in rats fed with the normal diet, it markedly attenuated hHcys-induced increase in O₂⁻ production in rats on the FF diet. These results are summarized in Figure 3C, showing that the FF diet increased glomerular O₂⁻ production by 1.84-fold and the administration of MK-801 significantly attenuated FF diet-enhanced O₂⁻ production. In addition, lipid peroxidation product (MDA + 4-HA) concentration was increased in the glomeruli of hHcys rats, which was blocked by the treatment with MK-801 (Fig. 3D).

TABLE 1. BODY WEIGHT, MAP, HEART RATE, HEMATOCRIT, AND RENAL FUNCTION DATA IN RATS FED WITH NORMAL DIET OR FF DIET WITH OR WITHOUT MK-801 TREATMENT

Parameter	ND N = 8	ND + MK-801 N = 7	FF N = 7	FF + MK-801 N = 8
Body weight (g)	444.75 ± 13.28	442.75 ± 22.24	461.06 ± 8.40	459.02 ± 11.06
MAP (mmHg)	106.76 ± 2.27	107.76 ± 1.41	104.41 ± 1.15	105.83 ± 2.53
Heart rate (beats/min)	341.29 ± 3.86	340.25 ± 6.35	351.35 ± 5.41	345.44 ± 8.27
Hematocrit (%)	50.40 ± 1.16	49.97 ± 1.10	47.97 ± 1.14	48.66 ± 1.09
Urinary output (ml)	10.05 ± 0.88	11.40 ± 1.42	13.92 ± 3.05	11.95 ± 2.64
Urine alb (mg/24h)	7.81 ± 1.22	6.84 ± 1.27	26.12 ± 3.80*	12.70 ± 2.55 [#]
Ccr (ml/min)	1.21 ± 0.09	1.12 ± 0.08	0.67 ± 0.02*	0.93 ± 0.04 [#]

Ccr, creatinine clearance; FF, folate-free diet; MAP, mean arterial pressure; ND, normal diet; Urine alb, urine albumin excretion. The data is expressed as mean ± SEM. * $p < 0.05$ as compared with ND; [#] $p < 0.05$ as compared with FF.

MK-801 administration attenuated glomerular injury and ECM deposition in hHcys rats

In parallel to elevated glomerular $O_2^{\cdot-}$ production, 24-h urinary albumin excretion was significantly increased in rats on the FF diet (Table 1). Morphological examinations showed pathological changes indicating glomerulosclerosis, such as capillary collapse and ECM deposition (Fig. 4A). The average glomerular damage index was significantly higher in these hyperhomocysteinemic rats (Fig. 4B). Masson trichrome staining showed that a 6-week FF diet treatment did not in-

duce a significant tubulo-interstitial fibrosis (Supplemental Fig. 2; see www.liebertonline.com/ars). In MK-801-treated rats, the same plasma Hcys level produced much less glomerular damage, as shown by less severe albuminuria and glomerular damage index, as well as improved creatinine clearance (Fig. 4B and Table 1).

To explore the mechanism of NMDA receptor in hHcys-induced glomerular damage, we determined collagen deposition in the glomeruli of hHcys rats. Using Sirius red as a dye for staining collagens, it was shown that collagen deposition in the glomeruli of hHcys rats were significantly increased as

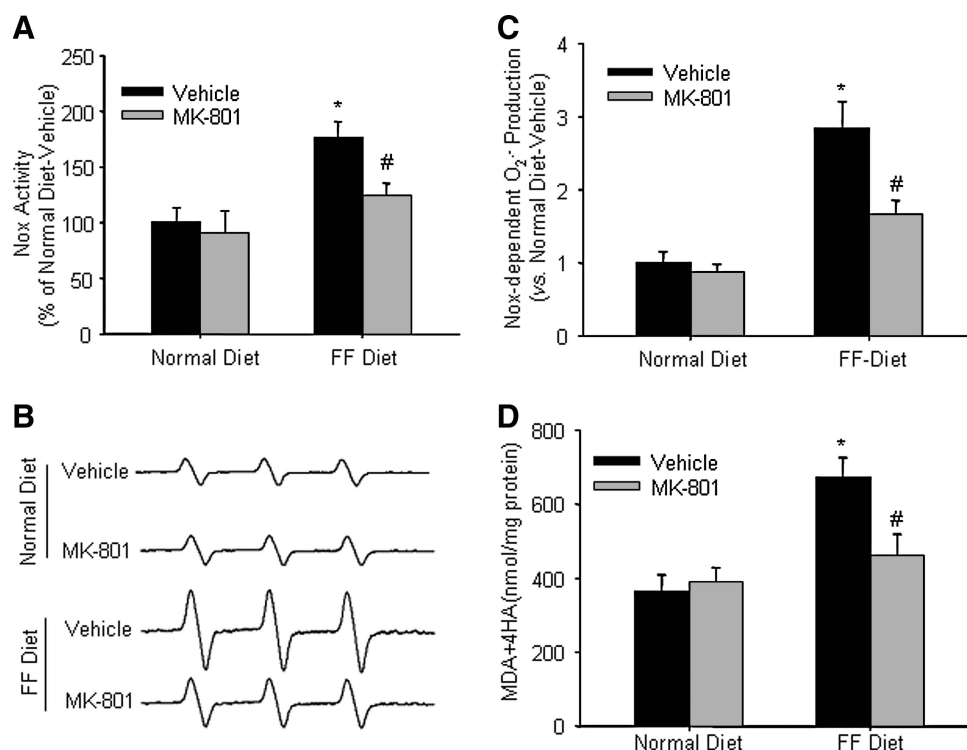


FIG. 3. Blocking the NMDA receptor by MK-801 reduced glomerular Nox activity, Nox-dependent $O_2^{\cdot-}$ production, and lipid peroxidation in hHcys rats. (A) Summarized DHE assay shows Nox activities in the glomeruli from rats on a normal or FF diet with or without MK-801 treatment. The data are expressed as percent changes in Nox activity compared with vehicle-treated rats on the normal diet. ($n = 5$ per group). (B) Representative ESR spectra traces for Nox-dependent $O_2^{\cdot-}$ production. (C) Summarized data show fold changes of Nox-dependent $O_2^{\cdot-}$ production in rat glomeruli, which are normalized to vehicle-treated rats on the normal diet (Normal diet, $n = 6$; other groups, $n = 8$). (D) Glomerular MDA + 4-HA concentrations in normal diet and FF diet rats maintained with or without MK-801 treatment ($n = 5$ per group). * $p < 0.05$ vs. rats on the normal diet; [#] $p < 0.05$ vs. vehicle-treated rats on the FF diet.

FIG. 4. MK-801 attenuated hHcys-induced glomerular injury and collagen deposition in rats with hHcys. (A) PAS staining shows glomerular morphological changes (original magnification, X400). (B) Summarized data of glomerular damage index (GDI) by semiquantitation of scores for PAS staining in four different groups of rats ($n=6$ in each group). (C) Sirius red staining shows collagen deposition in rat glomeruli (original magnification, X400). (D) Quantitative data of Sirius red staining by calculating the ratio of positively-stained area/total glomerular area ($n=6$ per group). * $p < 0.05$ vs. rats on the normal diet; # $p < 0.05$ vs. vehicle-treated rats on the FF diet. (For interpretation of the references to color in this figure legend, the reader is referred to the web version of this article at www.liebertonline.com/ars).

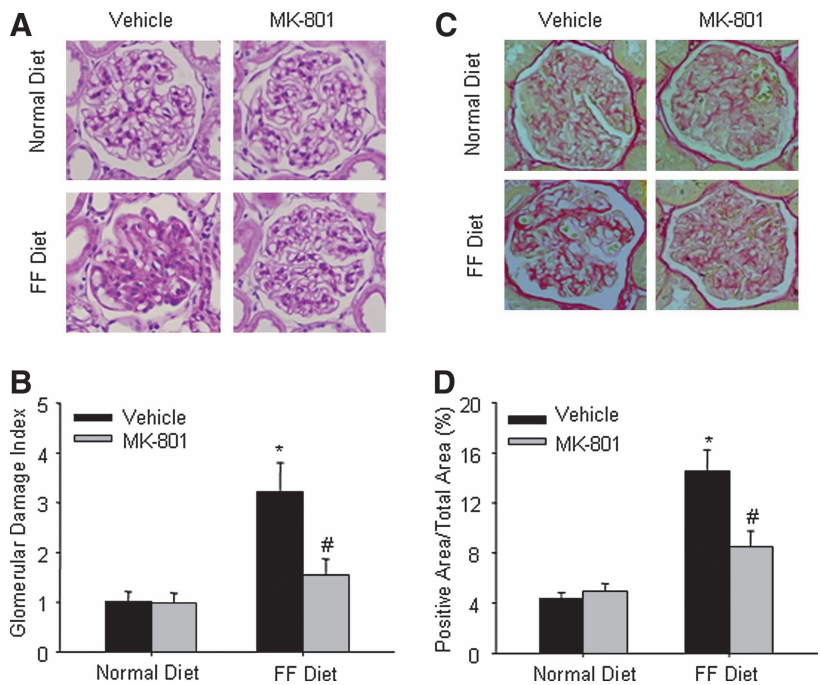
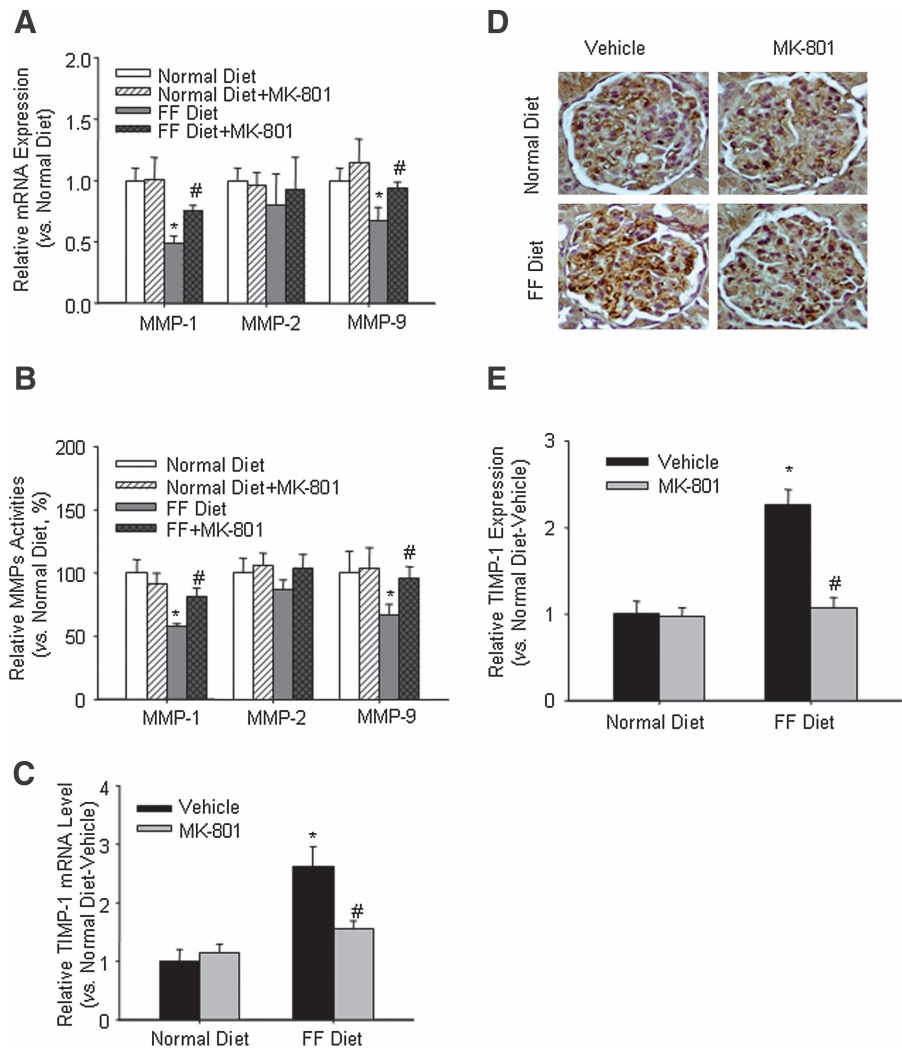


FIG. 5. Effects of MK-801 on MMP activities and TIMP-1 expression. (A) Changes in MMP-1, MMP-2, and MMP-9 mRNA expressions in the glomeruli detected by real-time RT-PCR ($n=5$ each). (B) MMP-1, MMP-2, and MMP-9 activities in isolated glomeruli were detected by FRET method ($n=7$ per group). (C) Real-time RT-PCR analysis of TIMP-1 mRNA expression in the glomeruli of different groups of rats ($n=6$ per group). (D) A representative immunohistochemistry image shows the expression of TIMP-1 in the glomeruli of different groups of rats (original magnification, X400). The area with brown color indicated positive staining for TIMP-1. (E) Quantitative analysis of TIMP-1 staining in the glomeruli. Data were normalized to vehicle-treated rats on the normal diet and the fold changes were compared. (Normal diet, $n=6$; other groups, $n=8$). * $p < 0.05$ vs. rats on the normal diet; # $p < 0.05$ vs. vehicle-treated rats on the FF diet. (For interpretation of the references to color in this figure legend, the reader is referred to the web version of this article at www.liebertonline.com/ars).



compared with those detected in rats on the normal diet. In rats treated with MK-801, however, hHcys-induced collagen deposition was significantly reduced (Figs. 4C and 4D).

Effects of MK-801 treatment on ECM metabolic enzymes in hHcys rats

To determine whether the protective effect of MK-801 on glomerular injury is associated with the changes in ECM metabolic enzymes, additional experiments were performed to examine the activities of the MMP family as well as the expression of TIMP-1 in the glomeruli from these rats. It was found that MMP-1 and MMP-9 mRNA expressions in the glomeruli from hHcys rats were markedly reduced, which could be restored by MK-801 treatment (Fig. 5A). Similar results were found in the activities of these enzymes as detected by FRET method (Fig. 5B). However, MMP-2 mRNA expression and activity were not changed in different groups of rats. TIMP-1, a major endogenous inhibitor of MMPs, was found to be increased by 1.8-fold in the glomeruli from rats on the FF diet. MK-801 treatment significantly blocked this Hcys-induced increase in the TIMP-1 level (Fig. 5C). Similarly, immunohistochemistry showed the same tendency in the protein expression of TIMP-1 in the glomeruli (Figs. 5D and 5E).

Effects of MK-801 on methionine-induced glomerular injury

To further clarify the protective effect of MK-801 in hHcys-induced glomerular injury, another hHcys animal model induced by methionine was used. As shown in Supplemental Figures 3A–3E (see www.liebertonline.com/ars), methionine treatment increased plasma Hcys levels, which was accompanied by significant increases in glomerular $O_2^{\cdot-}$ production and albumin excretion, as well as obvious glomerulosclerosis. All these pathophysiological changes induced by methionine were substantially blocked by the treatment with MK-801.

Pretreatment with MK-801 blocked L-Hcys-induced $O_2^{\cdot-}$ production in rat mesangial cells

Although we demonstrated in whole animal experiments that MK-801-treated rats were protected from hHcys-induced renal injury, it has yet to be determined whether such protective action is due to the direct action on glomerular cells. To address this issue and to explore potential underlying mechanisms, we examined the expression of NR1 and the changes in Nox-dependent $O_2^{\cdot-}$ production in *in vitro* cultured rat mesangial cells with and without pretreatment with MK-801 during Hcys exposure. As shown in Figures 6A and 6B, L-Hcys induced a significant increase in NR1 protein expression. ESR analysis showed that Nox-dependent $O_2^{\cdot-}$ production was doubled in L-Hcys-treated cells. Although MK-801 itself had no obvious effect on the basal level of $O_2^{\cdot-}$ production in these cells, it substantially reduced L-Hcys-induced increase in $O_2^{\cdot-}$ production (Figs 6C and 6D).

Effects of MK-801 on L-Hcys-induced changes in MMP-1 activity and TIMP-1 expression in rat mesangial cells

To examine whether the regulation of MMP-1, an important MMP in mesangial cells, is associated with the NMDA receptor during hHcys, MMP-1 activity was measured by

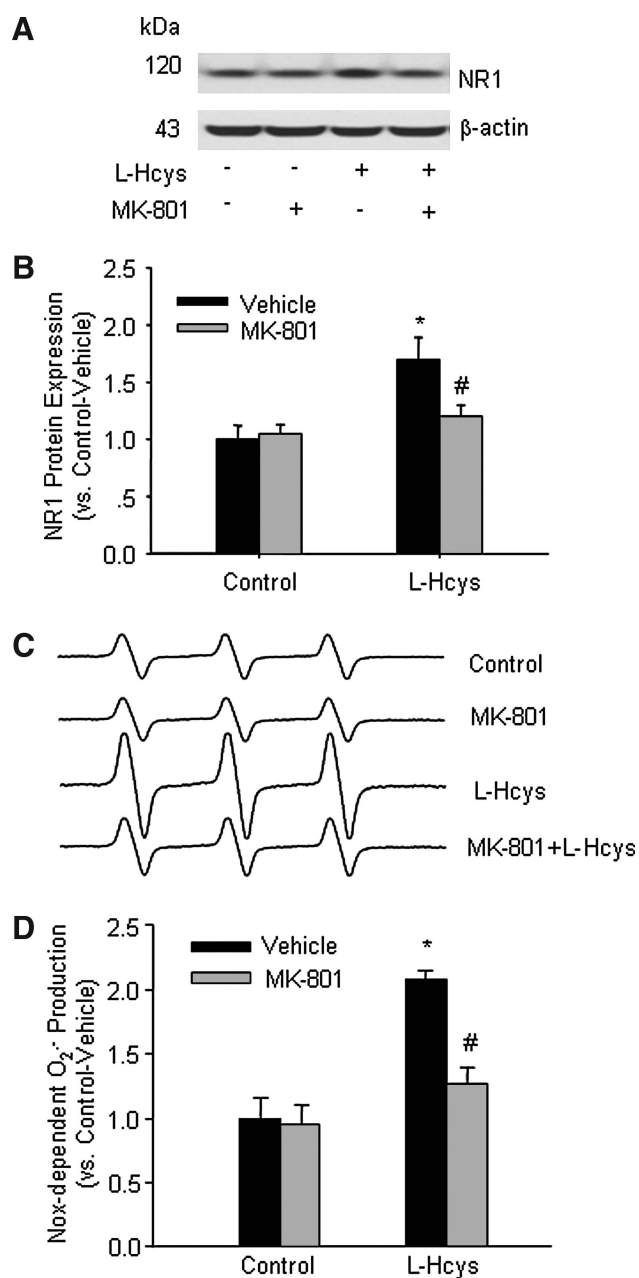
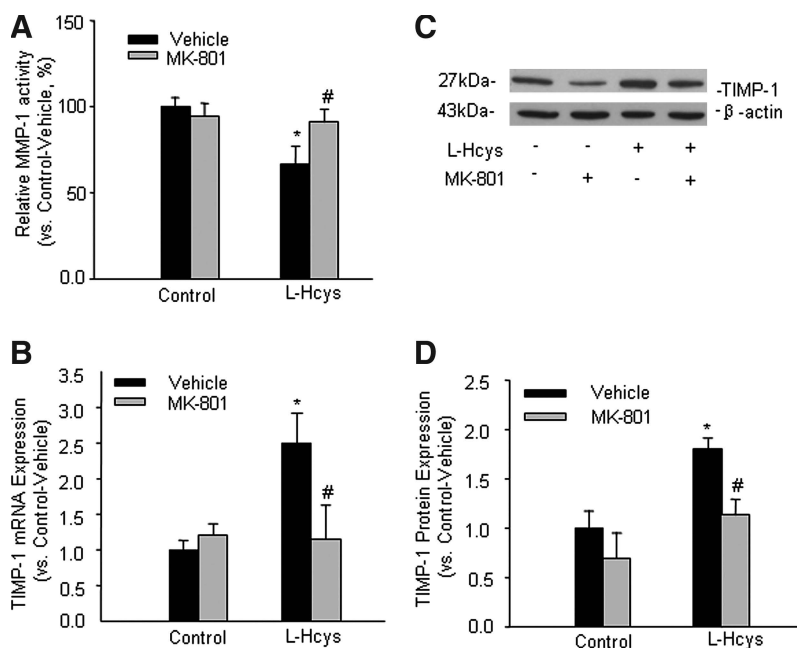


FIG. 6. Hcys-induced NR1 expression and $O_2^{\cdot-}$ production in rat mesangial cells. (A) A representative gel image shows the expression of NR1 in different groups. (B) Relative quantitation of protein expression for Western blot analysis from different groups of cells as indicated ($n = 4$ per group). (C) Representative ESR spectra traces from five independent experiments. (D) Summarized data shows the fold changes of $O_2^{\cdot-}$ production compared with the control group; $n = 5$ per group. * $p < 0.05$ vs. control group; # $p < 0.05$ vs. L-Hcys-treated cells.

FRET assay. Summarized data in Figure 7A showed that MMP-1 activity was markedly reduced in L-Hcys-treated cells, while MK-801 treatment significantly restored L-Hcys-reduced MMP-1 activity. In addition, Western blot analysis showed that the protein expressions of MMP-1 and MMP-9 were both decreased by the treatment with L-Hcys, which were substantially restored by pretreatment with MK-801

FIG. 7. Effects of MK-801 on MMP-1 activity and TIMP-1 expression in rat mesangial cells. (A) Summarized data show percentage changes in MMP-1 activity as compared with control cells. (B) Real-time RT-PCR analysis of TIMP-1 mRNA expression. The data are presented as the fold changes compared to control group of cells ($n = 5$ per group). (C) Western blot analysis of TIMP-1 expression in different groups of cells. (D) Relative quantitation of protein expressions for Western blot analysis from different groups of cells as indicated ($n = 5$ per group). * $p < 0.05$ vs. control group; # $p < 0.05$ vs. L-Hcys-treated cells.



(Supplemental Fig. 4; see www.liebertonline.com/ars). By real-time reverse transcription (RT)-PCR (Fig. 7B) and Western blot analysis (Figs. 7C and 7D), it was found that TIMP-1 mRNA and protein levels in L-Hcys-treated rat mesangial cells increased to 2.5-fold and 1.8-fold from the control level, respectively. However, MK-801 pretreatment significantly attenuated Hcys-induced increase in TIMP-1 expression.

Discussion

The major goal of this study is to determine whether the NMDA receptor is expressed in the glomeruli and mediates pathological actions of hHcys through the activation of Nox. We found that the NMDA receptor subunits, NR1 and NR2A, were expressed in the glomeruli and could be upregulated by hHcys, which was associated with increased Nox activity in the kidney and led to glomerulosclerosis. Using *in vitro* cultured mesangial cells, we demonstrated that NMDA receptor function is essential for Hcys-induced $O_2^{\cdot-}$ production and subsequent disturbance of the ECM metabolism. These results offer new evidence that the NMDA receptor may mediate Nox-dependent $O_2^{\cdot-}$ production induced by Hcys in mesangial cells and thereby play a crucial role in hHcys-induced glomerulosclerosis.

The NMDA receptor is comprised of various subunits, including NR1, NR2A, NR2B, NR2C, and NR2D. Each functional receptor contains at least one NR1 subunit, linking to either another NR1 subunit or any of NR2 subunits (23, 24). The NR1 subunit is the functional subunit that is essential for the channel activity, whereas the NR2 subunit confers modulatory properties (16). Although initially characterized in the brain, NMDA receptors are present in many other tissues outside the central nerve system, including the kidney. Some previous studies demonstrated the expression of NR1 and NR2C in renal tubules (18); however, the function of NMDA receptor in glomerular cells and its possible role in glomerulosclerosis have not been elucidated. By immunohisto-

chemical staining, we observed a clear expression of NR1 in the glomeruli. In contrast to our findings, a recent report showed that NR1 expression was mainly located in proximal tubular cells in Wistar rats (9). It is possible that species differences may lead to inconsistencies in the expression of NMDA receptor. In support of our current findings, Yang *et al.* (31) also demonstrated the presence of NR1 in the homogenate of rat glomeruli, although they did not specify which cell type expressed this subunit. We also found expression of NR2A both in the glomeruli and medulla, while there is no expression of NR2B detected under our experimental conditions. Since NR2C has been reported to be expressed only in renal tubular cells and NR2D to be absent in the rat kidney (18), we did not examine the expression of these subunits in the present study. Our results suggest that NR1 and NR2A are major NMDA receptor subunits in rat glomeruli.

Recent studies showed that the NMDA receptor is involved in various pathogenic actions during hHcys in neuronal cells (3), smooth muscle cells (2), and endothelial cells (6). Therefore, we went on to examine whether the NMDA receptor expression is influenced by hHcys in rat kidneys. Indeed, we found that the expressions of both NR1 and NR2A subunits were increased in the glomeruli of rats with hHcys, which could be inhibited by the treatment with MK-801, indicating the involvement of these NMDA receptors in the pathogenesis of hHcys-induced glomerular injury. Although there is a report indicating that Hcys-induced increase in NMDA receptor expression leads to sustained activation of the ERK pathway and results in neuronal cell death (26), the downstream mechanism mediating the pathogenic actions of NMDA receptor in the glomeruli remains unclear.

Given that oxidative stress has been implicated in the development of glomerular injury and end-stage renal disease, we hypothesized that the NMDA receptor may be associated with local oxidative stress in the kidney. In this regard, there are reports indicating that elevated Hcys level induces

oxidative injury in nerve terminals by stimulation of NMDA receptors and free radical formation (12). In our previous studies, we demonstrated that Nox-derived $O_2^{\cdot-}$ production is an important mechanism mediating hHcys-induced glomerular injury or damage (37). It is possible that hHcys-induced Nox activation is mediated by NMDA receptor. Indeed, our DHE assay and ESR data showed that the FF diet induced significant increases in Nox activity and Nox-dependent $O_2^{\cdot-}$ production in rat glomeruli, both of which were blocked by the treatment with a NMDA receptor antagonist, MK-801. In addition, hHcys-induced lipid peroxidation in the glomeruli was also blocked by MK-801 treatment. These results suggest the important role of the NMDA receptor in mediating $O_2^{\cdot-}$ production through the activation of Nox system in the kidney during hHcys. In accordance with lower $O_2^{\cdot-}$ production in MK-801-treated rats on the FF diet, urine albumin excretion was significantly decreased as compared with rats only receiving the vehicle, suggesting that local oxidative stress-associated renal injury during hHcys was alleviated by blocking the NMDA receptor. Our morphological examinations also support this view because a significant improvement of hHcys-induced glomerulosclerosis was observed in MK-801-treated rats.

Next, we explored the mechanisms activating the cascade of glomerulosclerosis by NMDA receptor in hHcys rats. It has been widely accepted that in spite of various initial insults to the glomeruli, ECM accumulation is a direct cause of glomerulosclerosis, which is characterized by increased production of collagens, fibronectin, and proteoglycans in injured glomeruli (21). We therefore examined collagen deposition in the rat kidneys. As expected, hHcys was found to increase collagen deposition in the glomeruli, and blocking the NMDA receptor with MK-801 substantially attenuated hHcys-induced accumulation of these collagens. This is consistent with a recent study showing that activation of the NMDA receptor may induce collagen deposition in neuronal and glial cells and thereby participate in the development of Alzheimer's disease and other neurodegenerative diseases (30).

In addition, we examined glomerular ECM metabolizing enzymes in the glomeruli of these rats. It is well known that MMPs/TIMPs are the major enzyme systems in regulating ECM degradation in the kidney. MMPs are predominantly responsible for degrading mature ECM, such as collagens and fibronectin, which are the major ECM components during glomerulosclerosis. TIMPs serve as tissue inhibitors of the MMP system, and their upregulation results in inhibition of MMPs activity and lowers ECM degradation rate (1). Our present study showed that glomerular MMP-1 and MMP-9 expressions and activities were decreased by hHcys while TIMP-1 expression was increased by hHcys, which were all reversed by blocking the NMDA receptor. These results highlighted the important role of NMDA receptor in modulating ECM degradation in the glomeruli during hHcys. Taken together, it appears that NMDA receptor-mediated $O_2^{\cdot-}$ production may play a crucial role in mediating hHcys-induced increase in ECM production and decrease in ECM degradation, which ultimately leads to glomerulosclerosis.

Although we have demonstrated that NMDA receptor blockade ameliorated hHcys-induced glomerular damage in the FF diet-treated animal model, there is a concern that this model might not disentangle the effects of folate deficiency from those of hHcys. To address this issue, a folate-sufficient

hHcys model induced by methionine was established. The data showed that, similar to FF diet-induced hHcys rats, MK-801 treatment decreased Nox-dependent $O_2^{\cdot-}$ production, alleviated albuminuria, and improved renal pathological changes. These findings further support our hypothesis that NMDA receptor is an essential mediator of hHcys-induced oxidative stress and glomerular injury. In contrast to our findings, a recent study done by Giardino and colleagues (14) showed that acute NMDA receptor blockade might cause damage to glomerular epithelial cells (*i.e.*, podocytes). Although the reasons for such discrepancy are not precisely known, differences in animal models and cell types, as well as the dosages of NMDA receptor blocker used in both studies may partially explain the inconsistencies between our findings and that study.

In addition to whole animal experiments, we also used cultured rat mesangial cells to examine the effect of blocking the NMDA receptor on Hcys-induced functional changes. Mesangial cells were chosen since these cells have been demonstrated to play a key role in the development of glomerulosclerosis, and many pathologic changes in the sclerotic glomeruli, such as increased matrix formation and proteoglycan aggregation, are associated with their dysfunction or damage (32). Our previous work have shown that expressions of Nox subunit, such as Rac1, was increased when mesangial cells were stimulated with Hcys (32, 33), indicating the important role of Nox activation in Hcys-induced injury in these cells. In the present study, ESR analysis showed that Hcys induced a significant enhancement of Nox-dependent $O_2^{\cdot-}$ production in cultured mesangial cells, which was blocked by the pretreatment with MK-801, suggesting that Hcys may produce Nox activation and oxidative stress through the NMDA receptor. Functionally, pretreatment of mesangial cells with MK-801 almost completely abolished Hcys-induced decrease in MMP-1 activity and increase in TIMP-1 expression. These results from cultured mesangial cells further confirm the findings from our *in vivo* studies, supporting the view that Hcys disturbs the homeostasis of ECM in mesangial cells through NMDA receptor-mediated activation of Nox and subsequent $O_2^{\cdot-}$ generation.

In summary, we demonstrated that Hcys-induced Nox activation and $O_2^{\cdot-}$ production in the glomeruli are mediated by the NMDA receptor, which causes increased deposition as well as decreased degradation of ECM components, leading to glomerulosclerosis. The amelioration of glomerular damage in hHcys rats by the NMDA receptor blocker, MK-801, further strengthened the important role of this receptor in hHcys-induced glomerulosclerosis. Therefore, these findings may potentially direct toward the development of new therapeutic strategies for treatment and prevention of end-stage renal disease associated with hHcys and hHcys-related pathological processes such as hypertension, diabetes, atherosclerosis, and aging.

Acknowledgments

This study was supported by grants DK54927, HL075316, and HL57244 from the National Institutes of Health.

Author Disclosure Statement

No competing financial interests exist.

References

1. Ahmed AK, Haylor JL, El Nahas AM, and Johnson TS. Localization of matrix metalloproteinases and their inhibitors in experimental progressive kidney scarring. *Kidney Int* 71: 755–763, 2007.
2. Au AL, Seto SW, Chan SW, Chan MS, and Kwan YW. Modulation by homocysteine of the iberiotoxin-sensitive, Ca²⁺-activated K⁺ channels of porcine coronary artery smooth muscle cells. *Eur J Pharmacol* 546: 109–119, 2006.
3. Bleich S, Degner D, Bandelow B, von Ahsen N, Ruther E, and Kornhuber J. Plasma homocysteine is a predictor of alcohol withdrawal seizures. *Neuroreport* 11: 2749–2752, 2000.
4. Bona KH, Njolstad I, Ueland PM, Schirmer H, Tverdal A, Steigen T, Wang H, Nordrehaug JE, Arnesen E, and Rasmussen K. Homocysteine lowering and cardiovascular events after acute myocardial infarction. *N Engl J Med* 354: 1578–1588, 2006.
5. Brown JC, Rosenquist TH, and Monaghan DT. ERK2 activation by homocysteine in vascular smooth muscle cells. *Biochem Biophys Res Commun* 251: 669–676, 1998.
6. Chen H, Fitzgerald R, Brown AT, Qureshi I, Breckenridge J, Kazi R, Wang Y, Wu Y, Zhang X, Mukunyadzi P, Eidt J, and Moursi MM. Identification of a homocysteine receptor in the peripheral endothelium and its role in proliferation. *J Vasc Surg* 41: 853–860, 2005.
7. Davies J, Evans RH, Francis AA, and Watkins JC. Excitatory amino acid receptors and synaptic excitation in the mammalian central nervous system. *J Physiol (Paris)* 75: 641–654, 1979.
8. Deng A and Thomson SC. Renal NMDA receptors independently stimulate proximal reabsorption and glomerular filtration. *Am J Physiol Renal Physiol* 296: F976–982, 2009.
9. Deng A, Valdivielso JM, Munger KA, Blantz RC, and Thomson SC. Vasodilatory N-methyl-D-aspartate receptors are constitutively expressed in rat kidney. *J Am Soc Nephrol* 13: 1381–1384, 2002.
10. Doronzo G, Russo I, Del Mese P, Viretto M, Mattiello L, Trovati M, and Anfossi G. Role of NMDA receptor in homocysteine-induced activation of mitogen-activated protein kinase and phosphatidylinositol 3-kinase pathways in cultured human vascular smooth muscle cells. *Thromb Res* 125: e23–32, 2010.
11. Ducloux D, Motte G, Challier B, Gibey R, and Chalopin JM. Serum total homocysteine and cardiovascular disease occurrence in chronic, stable renal transplant recipients: A prospective study. *J Am Soc Nephrol* 11: 134–137, 2000.
12. Dugan LL, Sensi SL, Canzoniero LM, Handran SD, Rothman SM, Lin TS, Goldberg MP, and Choi DW. Mitochondrial production of reactive oxygen species in cortical neurons following exposure to N-methyl-D-aspartate. *J Neurosci* 15: 6377–6388, 1995.
13. Folbergrova J. NMDA and not non-NMDA receptor antagonists are protective against seizures induced by homocysteine in neonatal rats. *Exp Neurol* 130: 344–350, 1994.
14. Giardino L, Armelloni S, Corbelli A, Mattinzoli D, Zennaro C, Guerrot D, Tourrel F, Ikehata M, Li M, Berra S, Carraro M, Messa P, and Rastaldi MP. Podocyte glutamatergic signaling contributes to the function of the glomerular filtration barrier. *J Am Soc Nephrol* 20: 1929–1940, 2009.
15. Ingram AJ, Krepinsky JC, James L, Austin RC, Tang D, Salapatek AM, Thai K, and Scholey JW. Activation of mesangial cell MAPK in response to homocysteine. *Kidney Int* 66: 733–745, 2004.
16. Ishii T, Moriyoshi K, Sugihara H, Sakurada K, Kadotani H, Yokoi M, Akazawa C, Shigemoto R, Mizuno N, Masu M, et al. Molecular characterization of the family of the N-methyl-D-aspartate receptor subunits. *J Biol Chem* 268: 2836–2843, 1993.
17. Leung JC, Marphis T, Craver RD, and Silverstein DM. Altered NMDA receptor expression in renal toxicity: Protection with a receptor antagonist. *Kidney Int* 66: 167–176, 2004.
18. Leung JC, Travis BR, Verlander JW, Sandhu SK, Yang SG, Zea AH, Weiner ID, and Silverstein DM. Expression and developmental regulation of the NMDA receptor subunits in the kidney and cardiovascular system. *Am J Physiol Regul Integr Comp Physiol* 283: R964–971, 2002.
19. Li N, Chen L, Yi F, Xia M, and Li PL. Salt-sensitive hypertension induced by decoy of transcription factor hypoxia-inducible factor-1 α in the renal medulla. *Circ Res* 102: 1101–1108, 2008.
20. Ma G, Allen TJ, Cooper ME, and Cao Z. Calcium channel blockers, either amlodipine or mibefradil, ameliorate renal injury in experimental diabetes. *Kidney Int* 66: 1090–1098, 2004.
21. Ma LJ and Fogo AB. Modulation of glomerulosclerosis. *Semin Immunopathol* 29: 385–395, 2007.
22. Mandir AS, Poitras MF, Berliner AR, Herring WJ, Guastella DB, Feldman A, Poirier GG, Wang ZQ, Dawson TM, and Dawson VL. NMDA but not non-NMDA excitotoxicity is mediated by Poly(ADP-ribose) polymerase. *J Neurosci* 20: 8005–8011, 2000.
23. Monyer H, Sprengel R, Schoepfer R, Herb A, Higuchi M, Lomeli H, Burnashev N, Sakmann B, Seeburg PH. Heteromeric NMDA receptors: Molecular and functional distinction of subtypes. *Science* 256: 1217–1221, 1992.
24. Moriyoshi K, Masu M, Ishii T, Shigemoto R, Mizuno N, and Nakanishi S. Molecular cloning and characterization of the rat NMDA receptor. *Nature* 354: 31–37, 1991.
25. Moustapha A, Gupta A, Robinson K, Arheart K, Jacobsen DW, Schreiber MJ, and Dennis VW. Prevalence and determinants of hyperhomocysteinemia in hemodialysis and peritoneal dialysis. *Kidney Int* 55: 1470–1475, 1999.
26. Poddar R and Paul S. Homocysteine-NMDA receptor-mediated activation of extracellular signal-regulated kinase leads to neuronal cell death. *J Neurochem* 110: 1095–1106, 2009.
27. Robinson K, Gupta A, Dennis V, Arheart K, Chaudhary D, Green R, Vigo P, Mayer EL, Selhub J, Kutner M, and Jacobsen DW. Hyperhomocysteinemia confers an independent increased risk of atherosclerosis in end-stage renal disease and is closely linked to plasma folate and pyridoxine concentrations. *Circulation* 94: 2743–2748, 1996.
28. Sen U, Basu P, Abe OA, Givvimani S, Tyagi N, Metreveli N, Shah KS, Passmore JC, and Tyagi SC. Hydrogen sulfide ameliorates hyperhomocysteinemia-associated chronic renal failure. *Am J Physiol Renal Physiol* 297: F410–419, 2009.
29. Tyagi N, Moshal KS, Sen U, Vacek TP, Kumar M, Hughes WM, Jr., Kundu S, and Tyagi SC. H₂S protects against methionine-induced oxidative stress in brain endothelial cells. *Antioxid Redox Signal* 11: 25–33, 2009.
30. Verdier Y, Zarandi M, and Penke B. Amyloid beta-peptide interactions with neuronal and glial cell plasma membrane: Binding sites and implications for Alzheimer's disease. *J Pept Sci* 10: 229–248, 2004.
31. Yang CC, Chien CT, Wu MH, Ma MC, and Chen CF. NMDA receptor blocker ameliorates ischemia-reperfusion-induced renal dysfunction in rat kidneys. *Am J Physiol Renal Physiol* 294: F1433–1440, 2008.

32. Yang ZZ and Zou AP. Homocysteine enhances TIMP-1 expression and cell proliferation associated with NADH oxidase in rat mesangial cells. *Kidney Int* 63: 1012–1020, 2003.
33. Yi F, Chen QZ, Jin S, and Li PL. Mechanism of homocysteine-induced Rac1/NADPH oxidase activation in mesangial cells: Role of guanine nucleotide exchange factor Vav2. *Cell Physiol Biochem* 20: 909–918, 2007.
34. Yi F, dos Santos EA, Xia M, Chen QZ, Li PL, and Li N. Podocyte injury and glomerulosclerosis in hyperhomocysteinemic rats. *Am J Nephrol* 27: 262–268, 2007.
35. Yi F, Xia M, Li N, Zhang C, Tang L, and Li PL. Contribution of guanine nucleotide exchange factor Vav2 to hyperhomocysteinemic glomerulosclerosis in rats. *Hypertension* 53: 90–96, 2009.
36. Yi F, Zhang AY, Janscha JL, Li PL, and Zou AP. Homocysteine activates NADH/NADPH oxidase through ceramide-stimulated Rac GTPase activity in rat mesangial cells. *Kidney Int* 66: 1977–1987, 2004.
37. Yi F, Zhang AY, Li N, Muh RW, Fillet M, Renert AF, and Li PL. Inhibition of ceramide-redox signaling pathway blocks glomerular injury in hyperhomocysteinemic rats. *Kidney Int* 70: 88–96, 2006.
38. Zhang C, Hu JJ, Xia M, Boini KM, Brimson CA, Laperle LA, and Li PL. Protection of podocytes from hyperhomocysteinemia-induced injury by deletion of the gp91(phox) gene. *Free Radic Biol Med* 48: 1109–1117, 2010.

Abbreviations Used

ECM = extracellular matrix
ELISA = enzyme-linked immunosorbent assay
ESR = electromagnetic spin resonance
FF = folate-free
FRET = fluorescence resonance energy transfer
GDI = glomerular damage index
Hcys = homocysteine
hHcys = hyperhomocysteinemia
HPLC = high-performance liquid chromatography
MK-801 = dizocilpine maleate
MMP-1 = matrix metalloproteinase-1
NMDA = N-methyl-D-aspartate
O ₂ ^{·-} = superoxide anion
PAS = periodic acid-Schiff
RT-PCR = reverse transcription polymerase chain reaction
TIMP-1 = tissue inhibitor of metalloproteinase-1

Address correspondence to:

Pin-Lan Li, M.D., Ph.D.

Department of Pharmacology and Toxicology

Medical College of Virginia

Virginia Commonwealth University

410 N 12th Street

Richmond, VA 23298

E-mail: pli@vcu.edu

Date of first submission to ARS Central, January 10, 2010; date of final revised submission, April 18, 2010; date of acceptance, April 21, 2010.